Nested Transition Path Sampling

Bolhuis, P.G.; Csányi, G.

DOI
10.1103/PhysRevLett.120.250601
Publication date
2018
Document Version
Final published version
Published in
Physical Review Letters

Nested Transition Path Sampling

Peter G. Bolhuis[1] and Gábor Csányi[2]
[1]Van 't Hoff Institute for Molecular Sciences, Universiteit van Amsterdam, Science Park 904, Amsterdam 1098 XH, The Netherlands
[2]Engineering Laboratory, University of Cambridge, Trumpington Street, Cambridge CB2 1PZ, United Kingdom

(Received 10 October 2017; published 20 June 2018)

We introduce a novel transition path (TPS) sampling scheme employing nested sampling. Analogous to how nested sampling explores the entire configurational phase space for atomistic systems, nested TPS samples the entire available trajectory space in one simulation. Thermodynamic and path observables can be constructed *a posteriori* for all temperatures simultaneously. We exploit this to compute the rate of rare processes at arbitrarily low temperature through the coupling to easily accessible rates at high temperature. We illustrate the method on several model systems.

DOI: 10.1103/PhysRevLett.120.250601

Rare events are ubiquitous in the physical sciences. Examples are elementary chemical reactions, crystal nucleation, protein conformational changes, surface rearrangements, thermally activated dislocation migration, and other diffusion processes in solids. Being comparatively infrequent, these events are notoriously difficult to assess using straightforward molecular dynamics simulation techniques. Enhanced sampling can alleviate this problem, but requires *a priori* knowledge of reaction coordinates [1,2]. Transition path sampling (TPS) circumvents this requirement by sampling from the distribution of trajectories that undergo the rare event [3,4]. TPS results in a collection of unbiased reactive trajectories that can be analyzed for mechanistic and kinetic information. Since its development 20 years ago TPS has been extended in many ways [5–9]. A drawback of TPS, common to many techniques that rely on molecular dynamics to compute phase space averages, is that it is difficult to obtain the temperature dependence of observables [10]. The obvious solution, to perform multiple TPS simulations at different temperatures and thus compute the temperature dependence explicitly, is computationally very expensive. Here we pursue a different route, and use nested sampling (NS) to compute the "density of states" of trajectory space, a temperature independent quantity from which observables at any temperate can be obtained. Nested sampling was invented in 2004 by John Skilling, first and foremost to allow efficient evaluation of evidence integrals in Bayesian inference [11–13]. It is widely used in astronomical data analysis [14]. The close correspondence between Bayesian inference and statistical mechanics suggested a natural application in the latter field. After an early demonstration on lattice models [15], it was adapted for materials modeling and enables the determination of pressure-temperature-composition phase diagrams in a single consistent set of simulations, even without any prior knowledge of the crystal structure of solid phases. Applications to date have ranged from Lennard-Jones (LJ) clusters [16–18] and hard spheres [19] to embedded atom models of aluminium and alloys [20], water and polymers [21], protein folding [22], and liquid-vapor phase transitions [23,24].

The aim of this Letter is to develop and test the nested sampling algorithm for dynamical trajectories. This will allow evaluating temperature-dependent dynamical observables, such as mechanisms and rates, from path ensembles obtained in a single simulation and without defining any reaction coordinate.

Briefly, nested sampling works by determining the density of states in configuration space corresponding to a probability measure at a given value of probability by generating K samples distributed uniformly in configuration space with the one-sided hard constraint on the corresponding probabilities all being above the given probability, and looking at the distribution of the samples' probabilities. In statistical mechanics, the log of the probability corresponds to the energy. In practice the density of states is determined iteratively, starting with configurations that have the highest energies (lowest probabilities), where MC moves decorrelate very quickly. In each iteration, the sample with the highest energy is removed from the pool, its energy is recorded, and it becomes the new energy threshold below which the uniform sampling distribution is reconstructed. This is done by cloning one of the existing samples (which are already uniformly distributed), and then the copy is decorrelated from its source by a Markov chain Monte Carlo or other dynamical procedure, the only requirement being that the process returns a new sample which is again uniformly distributed under the hard constraint. Since one sample is removed in each iteration, the phase space volume enclosed by the energy level corresponding to the hard constraint reduces by a factor of $\alpha = K/(K+1)$. The iterations are repeated until all the samples in the pool converge on a very small part of phase space. Throughout this Letter we use

"energy" to mean the total energy, as opposed to just the potential energy, which is often the controlling variable when NS is used to compute the configurational partition function.

The key facts that make NS efficient are (i) obtaining uniformly distributed samples is easy at high energies, and (ii) as the energy threshold is lowered, maintaining the approximately uniform distribution of an existing pool is easier than generating uniformly distributed samples completely from scratch. These statements remain approximately true even if the landscape is highly multimodal, since with enough samples in the pool, many modes will be sampled simultaneously. The "magic" of NS (shared with other density-of-states methods) happens in *a posteriori* analysis. Given the density of states $\Omega(E)$, we define the cumulative density of states as

$$\chi(E) = \int_{-\infty}^{E} \Omega(E')dE'. \tag{1}$$

Since each iteration in the NS procedure reduces the phase space by a factor α, the total cumulative density of states (volume of phase space) corresponding to the energy level E_n at iteration n is $\chi(E_n) = \alpha^n$, where the total phase space volume of the system under the initial energy constraint is normalized to 1 [25]. The first object of interest is the partition function

$$Z(\beta) = \int_{-\infty}^{\infty} \Omega(E) e^{-\beta E} dE. \tag{2}$$

We approximate the density of states by the finite difference of successive values of $\chi(E)$ and the above integral for the partition function by a discrete sum over the energy levels, giving

$$Z(\beta) \approx \sum_n (\alpha^n - \alpha^{n+1}) e^{-\beta E_n}. \tag{3}$$

Using this expression, all thermodynamics can be extracted from the list of successive energy levels $\{E_n\}$. The expectation value of an observable A is given by

$$\langle A(\beta) \rangle \approx \frac{1}{Z(\beta)} \sum_n A(\mathbf{x}_n)(\alpha^n - \alpha^{n+1}) e^{-\beta E_n}, \tag{4}$$

where $\mathbf{x}_n$ is the actual configuration with energy E_n removed from the pool at iteration n. For example, one can obtain the expected internal energy using the formula

$$U(\beta) = \frac{1}{Z(\beta)} \sum_n (\alpha^n - \alpha^{n+1}) E_n e^{-\beta E_n}, \tag{5}$$

and also the heat capacity as

$$C_V(\beta) = \beta^2 \left(\frac{1}{Z(\beta)} \sum_n (\alpha^n - \alpha^{n+1}) E_n^2 e^{-\beta E_n} - U(\beta)^2 \right). \tag{6}$$

The key point is that all observables are estimated at all temperatures using the density of states obtained in a single NS simulation. The accuracy with which an observable is obtained depends partly on how well the density of states is resolved, and partly on how well the K samples in the pool approximate the distribution of the observable near a given energy level. Both of these errors decrease with the usual $1/K^{1/2}$ scaling typical of stochastic methods. Apart from K, the other parameter that influences the accuracy of NS is the memory and length of the dynamical or Markovian process that is used to decorrelate the cloned copy at each iteration; however, in multimodal situations, convergence can only be reached by increasing K.

Transition path sampling is an MC scheme in the space of trajectories. One of the goals of TPS is to obtain a collection of trajectories that connect two stable states, A and B. Denoting a trajectory of length L by $\mathbf{x} = \{x_0, x_1, \ldots x_L\}$ with x_i the configuration's positions and momenta, the path ensemble distribution is given by $P_{AB}(\mathbf{x}) = \mathbb{1}_A(x_0) P(\mathbf{x}) \mathbb{1}_B(x_L)/Z_{AB}$, with $P(\mathbf{x})$ the unbiased path probability (determined by the underlying dynamics), and where the characteristic functions $\mathbb{1}_{A,B}(x)$ are unity when x is inside the state definition, and zero otherwise. The path partition function is $Z_{AB} = \int \mathcal{D}\mathbf{x} \mathbb{1}_A(x_0) P(\mathbf{x}) \mathbb{1}_B(x_L)$ The path probability $P(\mathbf{x}) \sim e^{-\beta E(x_0)} \prod_i^L p(x_i \to x_{i+1})$ is given by the underlying dynamics, where $p(x_i \to x_{i+1})$ is the short-time Markovian probability for a transition from the x_i to x_{i+1} step, and the first Boltzmann factor accounts for the canonical distribution of the energy [5–7]. A particularly simple expression is obtained for deterministic dynamics in the *NVE* ensemble, where these short time probabilities are delta functions, $Z_{AB} = \int \mathcal{D}\mathbf{x} e^{-\beta E(x_0)} \mathbb{1}_A(x_0) \mathbb{1}_B(x_L)$. Note that while the path ensemble is the canonical *NVT* ensemble, the dynamics is *NVE*. This is unusual but not a contradiction. For instance, the coupling to the heat bath can be so weak that the dynamics is essentially microcanonical on short time scales (that of the path) and only relaxes to constant temperature in the stable states, where dwell times are long. Other ensembles are possible, and are treated elsewhere [5–7].

TPS samples the path ensemble using the "shooting" MC move, which creates a trial trajectory by selecting a random time slice, or configuration x_i, and integrating the equation of motion backwards and forwards in time. This trial path is accepted if the path connects the stable states [26]. Intuitively, the move will lead to a high acceptance if the starting time slice is near the saddle point connecting the stable states. This move allows a lot of freedom in implementation, and many versions exist [6]. Here we use flexible length shooting, which halts the integration when

reaching a stable state. The path length fluctuates, and to obey detailed balance a correction factor based on the path length is needed [7].

Nested path sampling can now be constructed analogously to regular NS, making the identification

$$Z_{AB} = \int dE \int \mathcal{D}\mathbf{x} e^{-\beta E(x_0)} \mathbb{1}_A(x_0) \mathbb{1}_B(x_L) \delta(E - E(x_0)) \equiv \int dE e^{-\beta E} \Omega_{AB}(E), \tag{7}$$

which defines the path density of states as $\Omega_{AB}(E) = \int \mathcal{D}\mathbf{x} \mathbb{1}_A(x_0) \mathbb{1}_B(x_L) \delta(E - E(x_0))$. Now we proceed as outlined above. The nested TPS algorithm uses a pool of K paths that randomly populate trajectory space, under the extra condition that paths connect A and B. Just as in ordinary NS the trajectory space is reduced by a factor $\alpha = K/(K+1)$ when removing the path with the highest energy E_n at iteration n.

In addition to the usual thermodynamic quantities, it is easy to extract path observables, such as transformation mechanisms. For instance, the fraction of pathways traversing via a mechanism m is given by

$$f^m_{AB}(\beta) = \frac{1}{Z(\beta)} \sum_n (\alpha^n - \alpha^{n+1}) e^{-\beta E_n} \delta^m_n, \tag{8}$$

where $\delta^m_n = 1$ when path n follows mechanism m and zero otherwise. Any path observable can be evaluated in this way.

Of special interest are the rate constants, which are difficult to obtain for a rare event using brute force dynamics. TPS has a special procedure to compute rate constants, using integration along an order parameter [5]. Here we take a different route and link the rate at any temperature β to any other temperature β_0 via

$$\ln k(\beta) - \ln k(\beta_0) = \int_{\beta_0}^{\beta} d\beta' \frac{\partial \ln k(\beta')}{\partial \beta'}. \tag{9}$$

In TPS the rate constant is the time derivative of a correlation function $C(t) = \langle \mathbb{1}_A(x_0) \mathbb{1}_B(x_L) \rangle / \langle \mathbb{1}_A(x_0) \rangle$:

$$k = \frac{dC(t)}{dt} = \frac{\langle \mathbb{1}_A(x_0) \dot{\mathbb{1}}_B(x_L) \rangle}{\langle \mathbb{1}_A(x_0) \rangle}. \tag{10}$$

Taking logarithms and the derivative with respect to β gives

$$\frac{\partial \ln k(\beta)}{\partial \beta} = \frac{\partial \ln \langle \mathbb{1}_A(x_0) \dot{\mathbb{1}}_B(x_L) \rangle_{AB}}{\partial \beta} - \frac{\partial \ln \langle \mathbb{1}_A(x_0) \rangle}{\partial \beta}. \tag{11}$$

Carrying out the derivative yields, after rearranging,

$$\frac{\partial \ln k(\beta)}{\partial \beta} = -\langle E \rangle_{AB} + \langle E \rangle_A, \tag{12}$$

where the subscript AB denotes a path average over trajectories connecting A and B, and the subscript A denotes an average over trajectories starting in A, both of course at a given temperature setting. As stated above, all these ensemble averages are straightforward to evaluate after the NS run. In contrast, this approach using ordinary TPS would necessitate a separate simulation for each temperature on a fine grid of values [10].

In order to help understanding and build intuition, we first illustrate NTPS on a double-well potential in two dimensions with two different transition channels. We chose the following potential form [27]

$$V(x,y) = 4(x^2 + y^2 - 1)^2 y^2 - e^{-4[(x-1)^2 + y^2]} - e^{-4[(x+1)^2 + y^2]} + e^{8(x-1.5)} + e^{-8(x+1.5)} + e^{\alpha(y+0.25)} + 0.2e^{-8x^2},$$

with $\alpha = -4$ that makes the height of the two saddles unequal (approximately 1.1 and 0.9 above the minima). We initialized the ensemble of 50 path samples by starting from the linear path and deforming each by 10 000 shooting moves and the very high energy limit of 20. The paths were discretized to allow 200 time steps of size 0.05, and the number of shooting moves used to decorrelate the cloned path in each subsequent NTPS iteration was 1000. Figure 1 shows the potential as a heat map, as well as the paths generated during the NTPS run. At early iterations (black lines), the path energy is high, and many kinds of paths are sampled, with transitions between the two channels easily made. During the middle of the run (light gray lines), paths are confined to the channels, with very few switches between the two. Towards the end of the run (white lines), paths are confined to the top channel which has a lower barrier (even though it is significantly longer in terms of path length between the minima). Figure 1(c) shows a trivial order parameter (the y value at the midpoint of the path) that distinguishes the two channels, as a function of NTPS iteration. In the first 300 iterations, paths are not confined to the channels, and many different values are present. Between iterations 300 and 480, paths are mostly confined to the two channels, with just a couple of paths across the local maximum in between them, and after iteration 480, all paths follow the top channel.

The second illustration of NTPS is on a 2D Lennard-Jones cluster of 7 particles. This simple system was used as a test bed for the development of the TPS algorithm [4,28]. At low temperature the cluster has 4 metastable states (ignoring permutations) between which transformations can occur [29]. TPS can sample all transitions but here we focus on the transitions out of the ground state into any of the remaining three states.

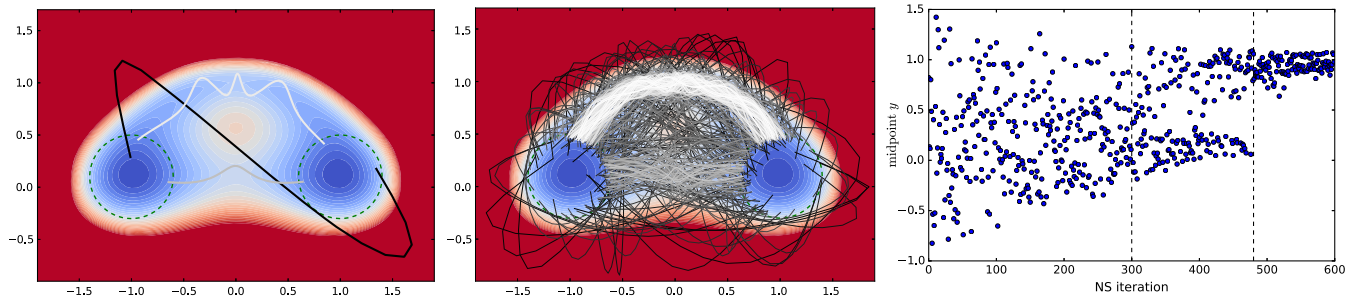

FIG. 1. (a) Double well potential with two transition channels. Three example paths are shown: a very high energy path (black) and two lower energy paths through the lower (gray) and upper (white) channels. (b)Nested transition path sampling of the double well potential. The brightness of the path indicates the NS iteration, with black corresponding to high energies and white paths to low energy paths. The green circles delimit the two states. (c) The y value at the path midpoint, as a function of NTPS iteration.

We initialize the ensemble of $K = 1000$ paths, performing l shooting moves between each sample. In each shooting move the velocities were changed with $dv_{\max} = 0.1$. To conserve the linear and angular momentum we applied a relative velocity change along a particle pair vector [30]. Paths connecting the ground state with any other metastable state are accepted. We restrict the energy of the NVE paths to a maximum of $E = -8.5$, as the acceptance probability vanishes at high energy, where the stable states are no longer basins of attraction. We obtained sufficiently decorrelated trajectories after $l = 1000$ shootings [31]. After the decorrelation phase, we apply the iterative nested sampling algorithm, using again $l = 1000$ shooting trials. This took around 24 hr on a single Intel CPU core. The cumulative density of states function in Fig. 2(a) shows that trajectory space is reduced by around 24 orders of magnitude during the nested sampling. From this data we construct the energy U via Eq. (5), shown in Fig. 2(b). As expected U decreases as function of inverse temperature β, eventually reaching the saddle point energy for $\beta \to \infty$. The heat capacity, which measures fluctuations in the path energy, is plotted in Fig. 2(c). C_V increases initially, indicating a rapid change in available path space, and settles to a constant value around $\beta \approx 20$, where the path energy fluctuations are completely determined by the saddle points. Figure 2(d) shows the probability of the observed mechanisms. Clearly, the transition to the higher lying metastable state becomes improbable at lower temperature, while the two other metastable states are about equally probable, which is reasonable considering the two saddle points are almost equal. At low β, these fractions differ from the simple prediction based on the Boltzmann factors of the barrier heights (dashed curves), indicating that entropy plays a role.

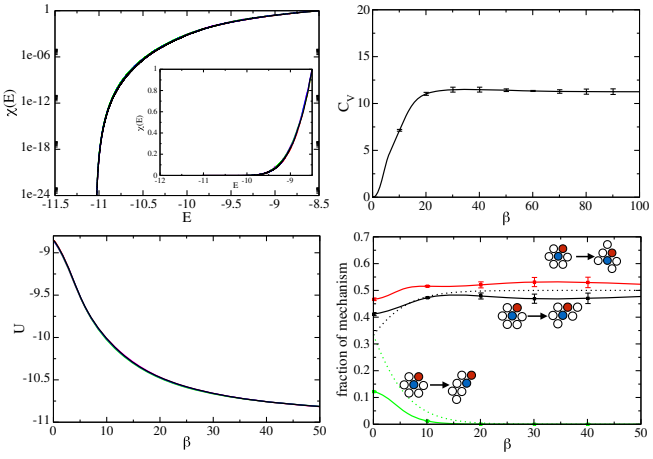

FIG. 2. NTPS of 2D LJ cluster transitions: (a) cumulative trajectory phase space volume $\chi(E)$, (b) internal energy, (c) heat capacity, and (d) fraction of paths following a given mechanism, all as functions of inverse temperature, β (solid curve). Fraction estimated from Boltzmann factor of saddle-point energy $E_s = -10.8$ (green dashed) and $E_s = -11.04$ (black dashed).

While we do not study the convergence with K here, we note that when NS is used to obtain the configurational partition function, K does not scale with system size directly, but with the number of relevant (symmetry reduced) energy basins that need separate sampling. The analog of that for NTPS is the number of different relevant transition mechanisms.

Next, we computed the derivative in Eq. (12) from the path observables. The unconstrained variable $\langle E \rangle_A$ was computed by carrying out a NTPS simulation of a path ensemble in which only the first slice was constrained to A. We integrate this derivative $d \ln k / d\beta$ (see inset in Fig. 3) using a known rate at high temperature β_0. Figure 3 shows the integrated NTPS rate for $\beta_0 = 10$. This known rate has to be computed directly at this high temperature, for instance using brute force MD. Figure 3 also shows computed rate constants at several other temperatures, including those from Refs. [28,29] for $\beta = 20$, indicating the NTPS prediction is excellent at low temperature. The direct computation becomes extremely slow around $\beta = 15$, while NTPS can easily assess rates up to $\beta = 50$. For $\beta < 6$ the direct MD rates deviate from the NTPS prediction, because of the imposed hard upper limit in energy. The NTPS estimate is only valid up to

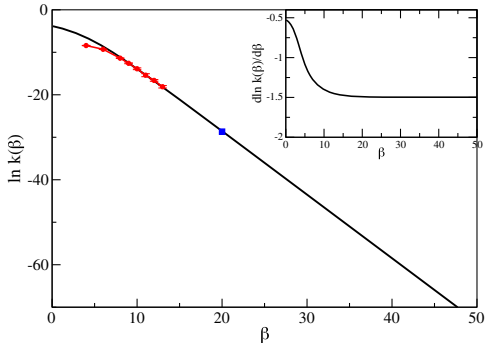

FIG. 3. Logarithm of rate constant of 2D LJ cluster transitions obtained by direct *NVT* MD (red circles), and by NTPS (black curve), integrated from the derivative shown in inset, with a reference temperature $\beta_0 = 10$. The blue square indicates rate constants for $\beta = 20$ taken from Refs. [28,29].

temperatures where the probability to observe this upper energy limit is negligible. The rate clearly shows Arrhenius behavior at high β, with the negative slope of the curve equal to the activation barrier, $E_a = -d \ln k/d\beta = 1.5$ (see inset of Fig. 3), which is indeed the barrier height [29].

In the above examples the effect of entropy is very limited, and in both cases Arrhenius behavior is observed. To show that NTPS also can handle barriers dominated by entropy, we provide a third example, a condensation transition in a small LJ system (see Supplemental Material [32]). This example clearly shows that when sampling the path density of states properly NTPS can correctly treat both energy as wells entropy dominated barriers.

In summary, we have introduced a novel path sampling method that uses the nested sampling algorithm to walk through trajectory space. We showed that rates can be obtained for all temperatures from a single simulation without defining a reaction coordinate. The nested transition path sampling method can be of interest when temperature dependence is required, which is difficult in ordinary TPS simulations. Finally, we note that the concept of nested sampling of path space is generally applicable to any thermal path integral, including quantum mechanical ones.

[1] *Free Energy Calculations: Theory and Applications in Chemistry and Biology: 86*, Springer Series in Chemical Physics, edited by C. Chipot and A. Pohorille (Springer, New York, 2007).

[2] T. Lelievre, G. Stoltz, and M. Rousset, *Free Energy Computations: A Mathematical Perspective* (Imperial College Press, London, 2010).

[3] C. Dellago, P. G. Bolhuis, F. S. Csajka, and D. Chandler, J. Chem. Phys. **108**, 1964 (1998).

[4] P. G. Bolhuis, C. Dellago, and D. Chandler, Faraday Discuss. **110**, 421 (1998).

[5] C. Dellago, P. G. Bolhuis, and P. L. Geissler, Advances in Chemical Physics Vol. 123 (John Wiley & Sons, Inc., Hoboken, NJ, 2002), p. 1.

[6] C. Dellago and P. G. Bolhuis, in *Advanced Computer Simulation Approaches for Soft Matter Sciences III*, edited by C. Holm and K. Kremer, Advances in Polymer Science Vol. 221 (Springer, Berlin, Heidelberg, 2009) p. 167.

[7] P. G. Bolhuis and C. Dellago, *Reviews in Computational Chemistry* (John Wiley & Sons, Inc., New York, 2010), Vol. 27, p. 111.

[8] P. G. Bolhuis and C. Dellago, Eur. Phys. J. Spec. Top. **224**, 2409 (2015).

[9] R. Cabriolu, K. M. S. Refsnes, P. G. Bolhuis, and T. S. van Erp, J. Chem. Phys. **147**, 152722 (2017).

[10] C. Dellago and P. G. Bolhuis, Mol. Simul. **30**, 795 (2004).

[11] J. Skilling, AIP Conf. Proc. **735**, 395 (2004).

[12] J. Skilling, J. Bayesian Analysis **1**, 833 (2006).

[13] J. Skilling, AIP Conf. Proc. **1193**, 277 (2009).

[14] F. Feroz and M. P. Hobson, Mon. Not. R. Astron. Soc. **384**, 449 (2008).

[15] I. Murray, D. J. C. MacKay, Z. Ghahramani, and J. Skilling, Adv. Neural Inf. Process. Syst. **18**, 947 (2006).

[16] L. B. Pártay, A. P. Bartók, and G. Csányi, J. Phys. Chem. B **114**, 10502 (2010).

[17] S. O. Nielsen, J. Chem. Phys. **139**, 124104 (2013).

[18] B. A. Wilson, L. D. Gelb, and S. O. Nielsen, J. Chem. Phys. **143**, 154108 (2015).

[19] L. B. Pártay, A. P. Bartók, and G. Csányi, Phys. Rev. E **89**, 022302 (2014).

[20] R. J. N. Baldock, L. B. Pártay, A. P. Bartók, M. C. Payne, and G. Csányi, Phys. Rev. B **93**, 174108 (2016).

[21] R. J. N. Baldock, N. Bernstein, K. M. Salerno, L. B. Pártay, and G. Csányi, Phys. Rev. E **96**, 043311 (2017).

[22] N. S. Burkoff, C. Várnai, S. A. Wells, and D. L. Wild, Biophys. J. **102**, 878 (2012).

[23] H. Do, J. D. Hirst, and R. J. Wheatley, J. Chem. Phys. **135**, 174105 (2011).

[24] H. Do, J. D. Hirst, and R. J. Wheatley, J. Phys. Chem. **116**, 4535 (2012).

[25] A different normalization would just result in a multiplicative constant in the partition function.

[26] The shooting move is known to be efficient in ordinary TPS, and since the *NVT* and *NVE* distributions are close for systems of moderate and high dimensionality, we expect it to be an efficient move for NTPS also.

[27] F. J. Pinski and A. M. Stuart, J. Chem. Phys. **132**, 184104 (2010).

[28] C. Dellago, P. G. Bolhuis, and D. Chandler, J. Chem. Phys. **108**, 9236 (1998).

[29] D. J. Wales, Mol. Phys. **100**, 3285 (2002).

[30] C. P. Lowe, Europhys. Lett. **47**, 145 (1999).

[31] Note that this is a much higher number of moves than reported in previous TPS applications where decorrelation is not required and 10 moves are typically adequate between recorded path samples.

[32] See Supplemental Material http://link.aps.org/supplemental/10.1103/PhysRevLett.120.250601 for an NTPS example on a simple system with an entropy dominated barrier, which includes Refs. [33–38].

[33] D. Frenkel and B. Smit, *Understanding Molecular Simulation, Second Edition: From Algorithms to Applications*, Computational Science Series (Academic Press, New York, 2001), Vol. 1.

[34] B. Smit, J. Chem. Phys. **96**, 8639 (1992).
[35] B. Peters and B. L. Trout, J. Chem. Phys. **125**, 054108 (2006).
[36] W.-N. Du and P. G. Bolhuis, J. Chem. Phys. **139**, 044105 (2013).
[37] W. Du and P. G. Bolhuis, J. Chem. Phys. **140**, 195102 (2014).
[38] W. Du and P. G. Bolhuis, Biophys. J. **108**, 368 (2015).